Journal of Colloid and Interface Science xxx (2013) xxx–xxx

Contents lists available at SciVerse ScienceDirect

Journal of Colloid and Interface Science

www.elsevier.com/locate/jcis

Electrokinetic concentration, patterning, and sorting of colloids with thin film heaters

Vanessa Velasco [a], Stuart J. Williams [a,b,*]

[a] Department of Mechanical Engineering, University of Louisville, Louisville, KY 40292, United States
[b] ElectroOptics Research Institute and Nanotechnology Center, University of Louisville, Louisville, KY 40292, United States

ARTICLE INFO

Article history:
Received 13 August 2012
Accepted 29 November 2012
Available online xxxx

Keywords:
Colloid self-assembly
Electrokinetics
Polarization
Electrothermal hydrodynamics
Dielectrophoresis

ABSTRACT

Reliable and simple techniques for rapid assembly and patterning of colloid architectures advance the discovery and implementation of such nanomaterials. This work demonstrates rapid electrokinetic two-dimensional assembly of colloidal structures guided by the geometry of thin film heaters within a parallel-plate device. This system is designed to enable either independently addressable or massively parallel colloidal assembly. A combination of electrothermal hydrodynamics, particle-electrode, and particle–particle electrokinetic interactions governs their assembly. Concentration and patterning of structures are shown with 1.0 μm polystyrene particles and sorting between 1.0 μm and 2.0 μm particles is demonstrated.

1. Introduction

Nanomanufacturing methods that can be implemented with standard engineering techniques will enable the discovery and development of novel nanomaterials and thereby bridge the gap between nanotechnology and manufacturing engineers and scientists. The development of break-through nanotechnologies for energy, thermal, optical, chemical, or mechanical materials requires high-volume production. There is a wide variety of micro- and nanometer-sized building blocks available (metals, oxides, semiconductors) and come in a range of shapes (rods, wires, etc.). Colloidal assembly techniques have generated custom architectures with enhanced physical properties; for example, such structures have been explored for optical applications including switches [1], optical sensors [2], photonic bandgap structures [3], and enhancement of solar cells [4]. A reliable self-assembly nanoparticle manipulation method that enables precise and rapid placement of colloids on a massive scale will provide an extremely valuable tool for the nanomanufacturing and development of novel materials.

The current challenge is shifting away from the creation of nanoparticles but rather toward their assembly and organization (1D, 2D, and 3D). Sedimentation methods [5,6] are generally hindered by lengthy colloid settling times and Brownian motion. Evaporation-induced assembly [7,8] is restricted to particles which sediment at a rate slower than the evaporation of the liquid, and sometimes, this method can take minutes to hours. Large-area monolayers [9,10] and template-assisted 2D architectures [11] are possible with evaporation. Electrokinetic methods have been incorporated to assemble colloids from partially-etched electrode patterns [12], excitation of photoconductive materials [13], or non-uniform electric fields [14]. However, electrokinetic particle-electrode attractive forces exponentially decrease with distance from the electrode surface. Further, other electrokinetic forces, like dielectrophoresis, are proportional to the cube of particle radius, further limiting its application to smaller colloids.

The method described within this paper is an adaptation of an optically induced electrokinetic method termed rapid electrokinetic patterning (REP) that can rapidly (seconds to minutes) concentrate hundreds of suspended colloids in packed, patterned aggregations [15–19]. Previous work used a near-infrared laser as a source of heating. Alternatively, this work uses micro-patterned thin film resistive heaters and offers numerous benefits over optical heating methods. Compared to optically-based REP, resistive heater methods are less expensive to operate, are more integratable with lab-on-a-chip technologies, are more energy efficient, and are scalable for manufacturing purposes.

Fig. 1 illustrates the operation of the thin film heater REP platform. The governed electrokinetic phenomena are driven with a set of parallel-plate electrodes generating a uniform AC field. One

Abbreviations: BOE, Buffered Oxide Etch; ITO, indium tin oxide; DEP, dielectrophoresis; REP, rapid electrokinetic patterning; PECVD, plasma enhanced chemical vapor deposition; DI, deionized.

* Corresponding author. Address: Department of Mechanical Engineering, 200 Sackett Hall, University of Louisville, Louisville, KY 40292, United States.
E-mail address: stuart.williams@louisville.edu (S.J. Williams).

0021-9797/$ - see front matter © 2012 Elsevier Inc. All rights reserved.
http://dx.doi.org/10.1016/j.jcis.2012.11.066

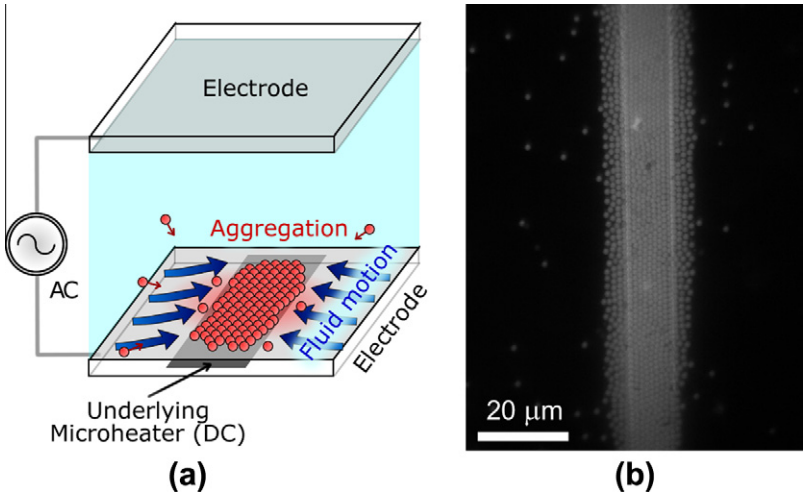

Fig. 1. (a) Illustration of REP driven by embedded, thin film resistive heaters. (b) Experimental result of 1.0 μm colloidal aggregation using a 10 μm wide resistive heater.

plate has an underlying array of patterned micrometer heaters, controlled by a DC signal, which are used to generate highly non-uniform temperature fields. The DC heaters are electrically insulated and isolated from the AC plate electrode. For colloidal assembly, a solution is introduced to the assembly region. Next, both the AC and the DC signals are activated. A combination of particle–particle, particle-electrode, and hydrodynamic electrokinetic phenomena results in rapid colloidal assembly. The aggregation geometry is defined by electrothermal hydrodynamics which are governed by the non-uniform temperature field. The novelty of this device is its ability to create 2D micrometer structures in parallel or in an independently addressable stepwise procedure with an array of heaters.

The governing physics of REP has been discussed previously [15,18]. This method is multidisciplinary in nature, including electrokinetics, heat transfer, fluid dynamics, and microfabrication. The physical mechanisms are illustrated in Fig. 2.

First, the DC heater is activated to generate non-uniform temperature fields. This contradicts traditional thin film heater design in typical microsystems where uniform temperature regions are generally desired. When the AC field is applied, electrothermal fluid motion is generated bringing suspended colloids toward the trapping region (Fig. 2I). The electrical permittivity (ε) and conductivity (σ) of fluids are temperature dependent, and fluid dielectric gradients are generated from non-uniform heating. As a result, a fluid body force will be exerted when an electric field is applied. The time-averaged expression for this body force (f_e) is [20]:

$$\langle f_e \rangle = 1/2Re\left[\frac{\sigma\varepsilon(\alpha-\beta)}{\sigma+i\omega\varepsilon}(\nabla T\cdot E)E^* - 1/2\varepsilon\alpha|E|^2\nabla T\right]$$

where Re refers the real part of the expression, E is the electric field, E^* is its complex conjugate, T is the temperature, ω is the applied frequency, σ and ε are the conductivity and permittivity of the fluid, respectively, β is $(1/\sigma)(\partial\sigma/\partial T)$, and α is $(1/\varepsilon)(\partial\varepsilon/\partial T)$. The first term is the Coulomb force, and the second term is the dielectric force. This expression is a function of the dielectric properties of the fluid and the applied AC signal. The fluid body force is dependent on local temperature gradients (∇T) – a larger body force is induced in areas of high temperature non-uniformity. Thermal gradients can be generated by Joule heating [20] or by illumination [21–23]. Here, the source of non-uniform heat comes from the micro-patterned DC heaters. Electrothermal fluid velocity (v) is proportional to the square of the electric field (E^2). Assuming Stokes' drag, the lateral force exerted on a particle is proportional to fluid velocity and particle radius (a). Other factors like hydrodynamic lifting forces (scaled as v^2) [24] and a particle's proximity to neighboring particles would influence these forces. However, additional electrokinetic forces acting on the colloids (Fig. 2II and III) overcome hydrodynamic lifting forces and trap particles on the electrode surface.

Successful REP aggregation is dependent on sharp temperature gradients rather than large overall temperatures. Optically induced temperature gradients of 0.2 °C per micrometer were achieved while trapping colloids with a maximum temperature of 7 °C [18]. REP electrothermal fluid motion is not natural convection,

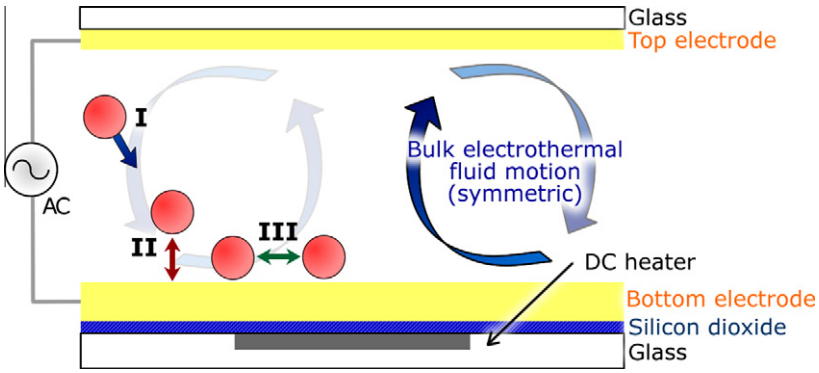

Fig. 2. Illustration of the physical mechanisms driving REP. Bulk electrothermal fluid motion (I) brings particles toward the electrode surface. When in close proximity to the electrode, AC electrokinetic particle-electrode holding forces (II) trap the particle close to the electrode surface. Particle–particle electrokinetic interactions (III) and bulk electrothermal fluid drag determine the nature of REP aggregation.

Please cite this article in press as: V. Velasco, S.J. Williams, J. Colloid Interface Sci. (2013), http://dx.doi.org/10.1016/j.jcis.2012.11.066

and colloid aggregation was not due to thermophoresis; when the AC field was deactivated (and heating remained active), fluid motion on the order of Brownian motion was observed, and particles did not accumulate [25].

As the electrothermal fluid drag carries the colloids toward the electrode surface (Fig. 2I), particle-electrode electrokinetic forces hold the particle near the electrode surface (Fig. 2II). These electrokinetic interactions have been investigated and are derived from a combination of particle-induced dielectrophoresis, localized AC electro-osmotic flow, electrostatic interactions, and van der Waals attraction [18,26–30]. Dielectrophoresis, by definition, occurs in a non-uniform electric field; in comparison, this system is inherently uniform. However, the particles themselves would distort the electric field leading to localized non-uniformities and, possibly, induce localized dielectrophoresis between the particle and the electrode. Localized AC electro-osmotic flow is induced due to the interaction of the applied electric field with the polarization of the ionic double layers of both the electrode and the particle. This polarization is attributed to the changes in surface charge density of the particle's electric double layer (EDL) whose polarization mechanism occurs at frequencies lower than the Maxwell–Wagner interfacial polarization [31].

In addition to particle-electrode attractive forces (Fig. 2II), there exist particle–particle electrokinetic interactions (Fig. 2III). The forces between particles can either be attractive or repulsive. Mutual particle attraction is the result of localized AC electro-hydrodynamics, whereas repulsive forces result from induced particle dipole–dipole interactions. These mechanisms are a function of AC frequency, electric field magnitude, particle size, electrolyte conductivity, and electrolyte type [30,32–34]. The electrothermal hydrodynamic drag (Fig. 2I) provides an additional, inward force component.

2. Materials and methods

2.1. Fabrication

Device fabrication started with a glass substrate, which was chosen over a silicon wafer for decreased thermal conductivity (k_{Si} = 149 W/(m-K), k_{glass} = 1.0 W/(m-K)), resulting in greater thermal heating efficiency. Next, photoresist was patterned through lithography to define the thin film heater geometry (Fig. 3a). The exposed glass was wet etched 200 nm (Fig. 3b) with a diluted solution of Buffered Oxide Etch (BOE); the etchant was diluted intentionally for a slower, controlled etch. After etching, a thin film of copper (200 nm) was deposited and patterned using lift-off photolithography, defining heater geometries that were near-flush with the glass surface (Fig. 3c). Next, a 1.0 μm layer of silicon dioxide was deposited through PECVD, providing an electric isolation layer between the copper heaters and the subsequent deposited layer of chrome/gold (30 nm/150 nm) (Fig. 3d). The silicon dioxide was etched in selective locations to allow electrical access to the heaters. The gold layer served as one side of the parallel-plate electrode, and an indium tin oxide (ITO) coated coverslip served as the opposite electrode. A 50 μm double-sided adhesive with microfluidic features separated the plates.

2.2. Temperature measurements

The temperature magnitude and field gradients generated from the thin film heaters were measured with an infrared microscope (InfraScope, QFI). This microscope has spatial resolutions of 1.5 μm. Assembled chips were filled with DI water before the application of DC voltages.

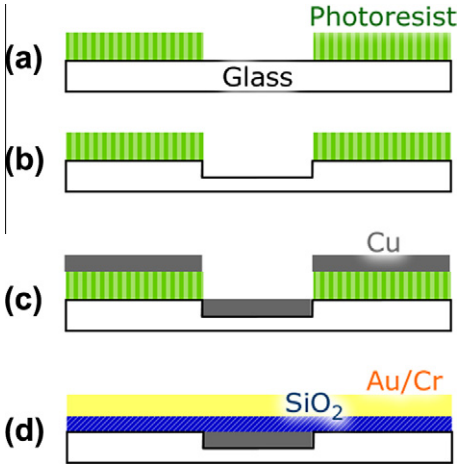

Fig. 3. Device fabrication began with (a) Photolithography of glass substrates, defining the geometry of the thin film heaters. (b) The exposed glass was wet etched to a depth of 200 nm with diluted BOE. (c) Next, 200 nm of copper was deposited, followed by removal of the photoresist. (d) Silicon dioxide (1 μm) was deposited followed by a patterned layer of chrome/gold (30 nm/150 nm). The oxide was removed in areas to allow electrical access to the underlying resistors.

2.3. Particle preparation

Approximately four drops of 1.0 μm red fluorescent particles (1% solids, Thermo Scientific) were diluted in 5 mL of DI water (0.27 mS/m), resulting in a particle concentration of approximately 3×10^8 particles per milliliter. Approximately eight drops of 2.0 μm red fluorescent particles (1% solids, Thermo Scientific) were diluted in 5 mL of DI water, resulting in a particle concentration of 0.75×10^8 particles per milliliter. Samples of 1.0 μm and 2.0 μm were combined for REP sorting experiments. Although DI water is used for this investigation, REP has been demonstrated with solutions at conductivities of 2.5 mS/m [19]. Previous investigations have demonstrated that REP performs best with low conductivity solutions. Local AC electro-osmotic flow, which is responsible for particle-electrode holding forces (Fig. 2II), is negligible at high AC frequencies and high fluid conductivities [35].

2.4. Image acquisition

The device was mounted on a Nikon Eclipse Ti inverted microscope; therefore, particle aggregation occurred on the upper electrode with respect to gravity. Fluorescent illumination was supplied from an X-Cite 120 Fluorescence System and passed through an excitation filter cube allowing green light be reflected off a dichroic mirror. The green illumination was delivered to the sample which excited the red fluorescent particles. Fluorescent images and videos were acquired by a high performance 12-bit CCD camera (SensiCAM QE, PCO).

3. Results and discussion

Heater geometries consisted of a larger wire trace width (100 μm) narrowing to 10 μm for a length of 200 μm. Although constant current runs throughout a single wire, the maximum heating occurs at narrow features. Wire heating is proportional to the square of the current density; therefore, a film geometry that is reduced to 1/10th of its width will experience 100 times more heating. Proper design and heat transfer of the thin film heaters are critical to control the behavior of electrothermal hydrodynamics for successful colloidal trapping and patterning. Fig. 4 shows the resultant temperature field for a single thin film trace at 1.6 V_{DC}

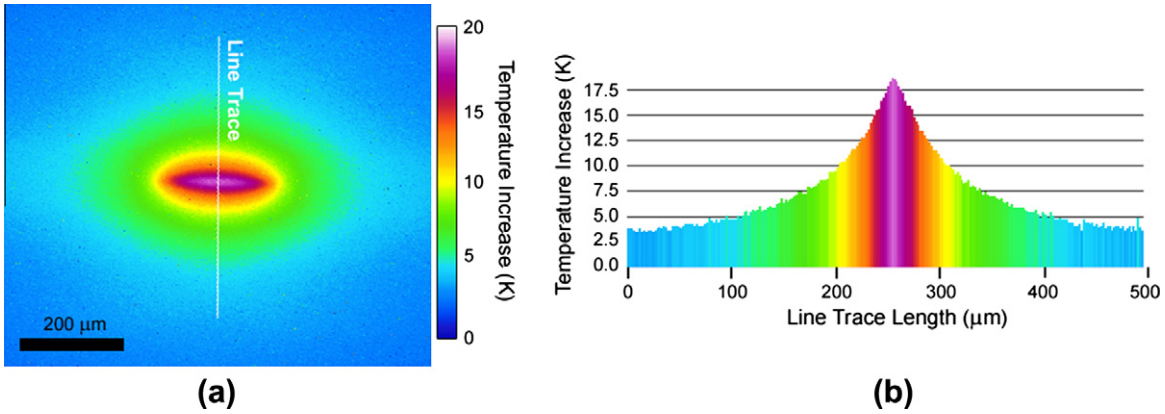

Fig. 4. (a) A top-view of the heating of a thin film heater narrowing to a 10 µm trace 200 µm long at 1.6 V_{DC}. (b) A cross-section of the temperature profile, demonstrating the gradient in temperature.

(59 mA); the maximum temperature increase and temperature gradient was 18 °C and 0.5 °C/µm, respectively. Subsequent experimental images and videos were acquired at 1.6 V_{DC} to demonstrate the particle trapping, patterning, and sorting capabilities of this device. However, colloidal aggregation can occur at lower temperatures. Trapping occurred at voltages as small as 0.8 V_{DC}, corresponding to a maximum temperature of 4.5 °C, though the rate of aggregation decreased with slower electrothermal microfluidic velocity (results not shown).

A three-dimensional electrothermal vortex was generated when the uniform AC field was applied simultaneously with heater activation. For the line heater geometry (Fig. 4), the fluid circulated inward along the surface of the heater-side planar electrode. Fluid motion resembled a slender elliptical vortex (a video showing this microfluidic circulation is available in Supplemental Information). At AC frequencies 200 kHz and greater, no particle accumulation was observed, though microfluidic motion was present. However, colloid trapping did occur at lower frequencies. Fig. 5 shows the trapping and patterning of 1.0 µm colloids with the line heater geometry at 1.6 V_{DC}, 10 V_{pp}, and 100 kHz; a video showing this accumulation is available in Supplemental Information. The shape of the colloidal aggregation resembled the thin film heater geometry as inward fluid motion corralled the particles on the electrode surface. The particle-electrode holding force was sufficient to keep the trapped colloids on the surface of the electrode instead of being carried away by the microfluidic vortex. The aggregation consisted of a monolayer of particles within the early stages of trapping; however, as more colloids were trapped a secondary and tertiary layer formed near its center. A second-layer colloid would position itself on top of three underlying colloids forming a local triangular tetrahedron due to a combination of reduced drag and attractive dipole–dipole interactions.

The nature of REP aggregation, including the layering and spacing between neighboring particles, has been investigated previously and is a function of fluid velocity, heating, and the applied AC signal [15,18]. The following is a brief discussion of these results, which were similarly observed for the resistive heater REP device. Fluid velocity was proportional to the square of the applied AC voltage, which follows theory of externally-heated electrothermal hydrodynamic devices. With increasing applied external heat, the microfluidic vortex velocity would increase, leading to faster aggregations and closer packed assemblies. However, during excessive heating, the electrothermal fluid velocity generated increases to the point where hydrodynamic drag and lift would deter particle aggregation. If the AC voltage was increased, the electrothermal velocity would increase, the rate of particle capture would increase, and the overall number of trapped particles would increase [15]. REP aggregations would occur for a range of AC frequencies between 1–200 kHz. At lower frequencies, localized AC electro-osmosis caused by adhered particles or imperfections on

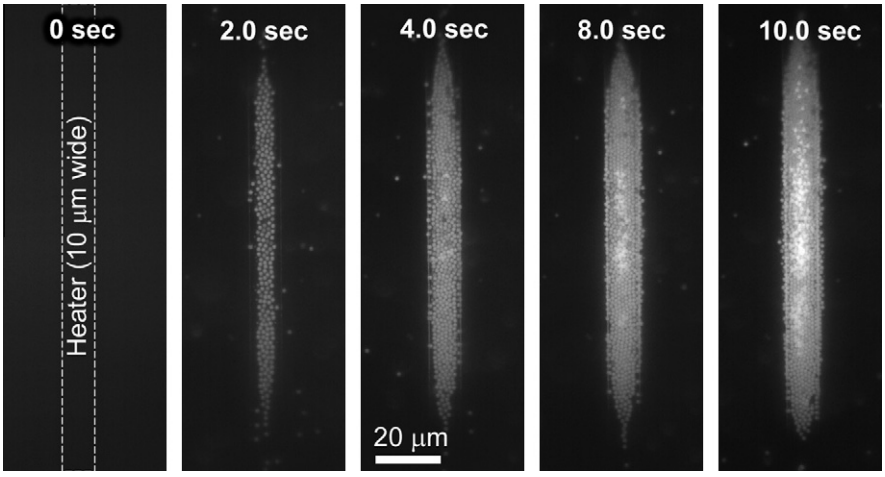

Fig. 5. These series of images demonstrate the rate and nature at which suspended 1.0 µm polystyrene particles were captured on a single heater (1.6 V_{DC}). The applied AC signal is 10 V_{pp} and 100 kHz.

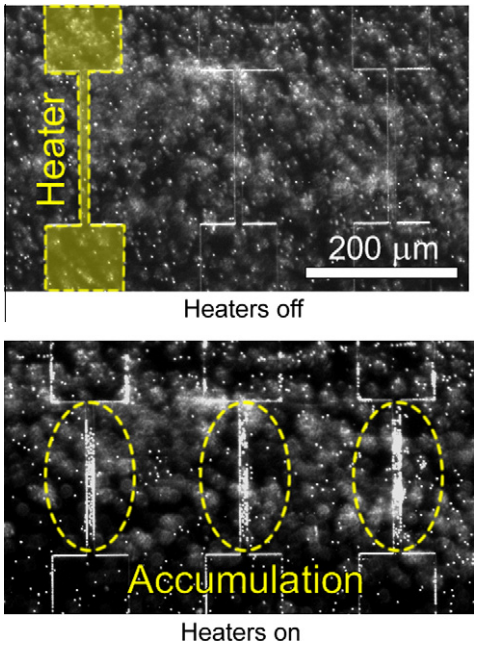

Fig. 6. Simultaneous electrokinetic colloid assembly at three thin film heaters (1.6 V_{DC}, 10 V_{pp}, 61 kHz).

the electrode surface would dominate electrothermal flow, drawing colloids away from the desired aggregation region. Particles would disperse at higher AC frequencies. Though the exact nature of particle release at high AC frequencies is not known, it has been demonstrated that the dispersion frequency of a colloid is inversely proportional to the square of its radius [15,18]. It is hypothesized that the polarization of the colloid's EDL plays a key role, as its dispersion, in its most simplified model [31], shows the same relaxation trend. Therefore, as the AC frequency is increased, larger particles would be released from the particle cluster before smaller particles. In addition, larger fluid conductivities would decrease the highest observed holding AC frequency, as larger fluid conductivities would mask the polarization effects of the EDL.

Next, an array of heater sites was designed to demonstrate parallel REP on the same device. With an array of independently addressable thin film heaters, the end user can initialize colloid self-assembly at one or more sites. Fig. 6 demonstrates simultaneous colloid assembly at three different sites with 1.6 V_{DC}, 10 V_{pp}, and 61 kHz. There has to be careful consideration when designing and operating an array of thin film REP devices. If two neighboring active heaters are too close in proximity of each other, their heated areas may overlap, resulting in a decreased temperature gradient between them. Smaller temperature gradients lead to slower electrothermal fluid velocities and, therefore, less compact and ill-defined colloid assemblies. An arrayed, independently addressable REP system could also be used to systematically transport colloidal aggregations in a stepwise procedure to different locations within a microsystem.

The REP aggregation resembles the geometry of the heater due to the generated electrothermal hydrodynamics. To illustrate the patterning capabilities further, an 'X'-shaped heater was fabricated with 10 μm wide traces (Fig. 7a). Fig. 7b shows the resultant temperature profile when two adjacent electrodes were connected to a 1.6 V_{DC} supply, and the other electrodes were grounded. The temperature gradient on the heater's inside corners becomes less sharp as you approach the center of the 'X' due to heat transfer and conduction. This is reflected in the resultant 1.0 μm colloid aggregation (Fig. 7c) at 1.6 V_{DC}, 10 V_{pp}, and 110 kHz.

This 'X' shape provides a representation of REP patterning capabilities, though its resolution could be improved. First, the design and incorporation of specific materials with proper heat transfer properties may generate sharper temperature gradients. Second, the otherwise planar electrode could be micro-patterned through partial or complete etching [12]. This would create non-uniform electric fields, introducing dielectrophoresis and AC electrohydrodynamics. These non-uniform electrokinetics would provide additional forces to confine and shape REP-trapped colloids.

Sorting experiments were conducted with 1.0 and 2.0 μm particles and results complement previous optically-based REP sorting demonstrations [15,18]. Initially, only 1.0 μm particles are captured at 1.6 V_{DC}, 100 kHz, and 10 V_{pp} (Fig. 8a). The 2.0 μm particles are present and circulate with the microfluidic vortex in close proximity to the line heater, though the particle-electrode holding forces are not sufficient to trap these larger particles at 100 kHz. Next, the AC frequency is changed to 50 kHz which is sufficient to trap the 2.0 μm particles and retain the 1.0 μm colloids (Fig. 8b). When the frequency is returned to 100 kHz, the 2.0 μm particles are released, while the 1.0 μm particles remain (Fig. 8c). A video of this sorting experiment is available in Supplementary Information.

There exists a critical AC frequency at which particles are no longer captured with REP. For similar particles, the critical frequency is inversely proportional to the diameter of the particle [15], which corresponds to Schwarz's fundamental model of the relaxation polarization of a colloid's electric double layer [31]. A

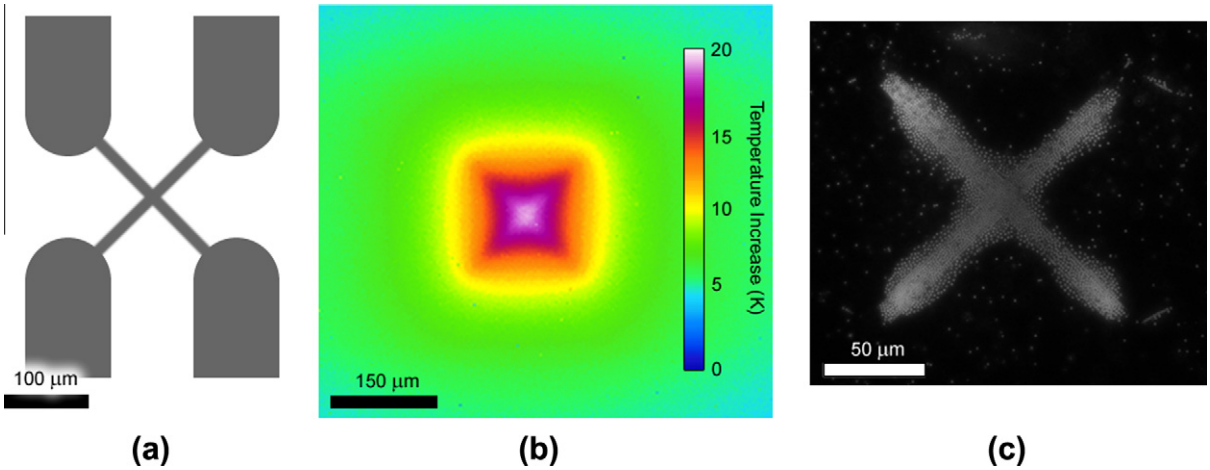

Fig. 7. The (a) design, (b) temperature profile, and (c) 1.0 μm colloid aggregation of an 'X'-shaped REP thin film heater at 1.6 V_{DC}, 10 V_{pp}, and 110 kHz.

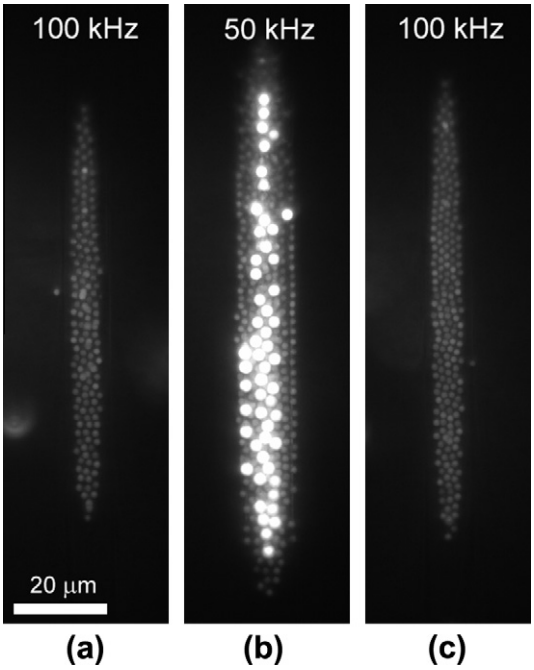

Fig. 8. (a) Initially, 1.0 μm particles are initially captured with REP at 1.6 V_{DC}, 10 V_{pp}, and 100 kHz. (b) 2.0 μm particles are captured at 50 kHz but (c) are released at 100 kHz, while retaining 1.0 μm particles.

more in-depth investigation into the underlying physics of REP particle release is necessary, as colloid double layer polarization and relaxation are a function of its composition and mobility. Theoretically, colloids with different surface chemistries can be sorted with REP and could be incorporated with analytical lab-on-a-chip systems.

4. Conclusions

This work demonstrates the fabrication and operation of an electrokinetic device capable of the rapid assembly of colloids using thin film resistive heaters. Previously, a single point-source trapping source has trapped hundreds of particles in minutes [15]. Thin film heaters expand the trapping area through their larger shape and addressable arrays. Patterning of colloid assemblies is governed by electrothermal hydrodynamics, and an assortment of geometries can be incorporated on the same REP platform. The use of resistive heaters has a thermal efficiency close to 100% (electrical energy conversion to heat energy). This is greater than optically induced heating methods, in which there is in inherent loss of optical power in the delivery of the laser to the system. Further, the creation of thin film heaters involves established microfabrication procedures, leading to straight-forward fabrication and potential incorporation with other microsystem devices. Here, the trapping and patterning of 1.0 μm particles were demonstrated; however, based on previous results [17], trapping of nanoparticles (50 nm) is possible. This method demonstrates a straightforward electrokinetic technique to concentrate, pattern, and sort particles in an independently addressable or massively parallel manner.

Funding sources

Start-up funds from the University of Louisville.

Acknowledgments

V. Velasco acknowledges the support of the Southern Regional Education Board's Doctoral Scholarship. S.J. Williams acknowledges the support from start-up funds from the University of Louisville.

Appendix A. Supplementary material

Supplementary data associated with this article can be found, in the online version, at http://dx.doi.org/10.1016/j.jcis.2012.11.066.

References

[1] J.M. Weissman, H.B. Sunkara, A.S. Tse, S.A. Asher, Science 274 (5289) (1996) 959–960.
[2] J.H. Holtz, S.A. Asher, Nature 389 (6653) (1997) 829–832.
[3] Y.N. Xia, B. Gates, Y.D. Yin, Y. Lu, Adv. Mater. 12 (10) (2000) 693–713.
[4] B. O'Regan, M. Gratzel, Nature 353 (1991) 737–740.
[5] A. van Blaaderen, R. Ruel, P. Wiltzius, Nature 385 (1997) 321–324.
[6] M. Holgado, F. Garcia-Santamaria, A. Blanco, M. Ibisate, A. Cintas, H. Miguez, C.J. Serna, C. Molpeceres, J. Requena, A. Mifsud, F. Meseguer, C. Lopez, Langmuir 15 (14) (1999) 4701–4704.
[7] E. Adachi, A.S. Dimitrov, K. Nagayama, Langmuir 11 (4) (1995) 1057–1060.
[8] N.D. Denkov, O.D. Velev, P.A. Kralchevsky, I.B. Ivanov, H. Yoshimura, K. Nagayama, Langmuir 8 (12) (1992) 3183–3190.
[9] H.-Y. Ko, H.-W. Lee, J. Moon, Thin Solid Films 30 (2004) 638–644.
[10] T.P. Bigioni, X.-M. Lin, T.T. Nguyen, E.I. Corwin, T.A. Witten, H.M. Jaeger, Kinetically driven self assembly of highly ordered nanoparticle monolayers, Nat. Mater. (2006) 265–270.
[11] N.N. Khanh, K.B. Yoon, J. Am. Chem. Soc. 131 (40) (2009) 14228–14230.
[12] W.D. Ristenpart, P. Jiang, M.A. Slowik, C. Punckt, D.A. Saville, I.A. Aksay, Langmuir 24 (2008) 12172–12180.
[13] R.C. Hayward, D.A. Saville, I.A. Aksay, Nature 404 (6773) (2000) 56–59.
[14] S. Kim, R. Asmatulu, H.L. Marcus, F. Papadimitrakopoulos, J. Colloid Interface Sci. 354 (2011) 448–454.
[15] S.J. Williams, A. Kumar, N.G. Green, S.T. Wereley, J. Micromech. Microeng. (2010) 20.
[16] S.J. Williams, A. Kumar, S.T. Wereley, Lab Chip 8 (2008) 1879–1882.
[17] S.J. Williams, A. Kumar, S.T. Wereley, Nanoscale 1 (1) (2009) 133–137.
[18] A. Kumar, J.-S. Kwon, S.J. Williams, N.G. Green, N.K. Yip, S.T. Wereley, Langmuir 26 (7) (2010) 5262–5272.
[19] V. Velasco, A.H. Work, S.J. Williams, Electrophoresis (2012) 33.
[20] N.G. Green, A. Ramos, A. Gonzalez, A. Castellanos, H. Morgan, J. Electrostat. 53 (2) (2001) 71–87.
[21] N.G. Green, A. Ramos, A. Gonzalez, A. Castellanos, H. Morgan, J. Phys. D-Appl. Phys. 33 (2) (2000) L13–L17.
[22] A. Mizuno, M. Nishioka, Y. Ohno, L.D. Dascalescu, IEEE Trans. Ind. Appl. 31 (3) (1995) 464–468.
[23] M. Nakano, S. Katsura, G.G. Touchard, K. Takashima, A. Mizuno, IEEE Trans. Ind. Appl. 43 (1) (2007) 232–237.
[24] P. Cherukat, J.B. McLaughlin, J. Fluid Mech. 263 (1994) 1–18.
[25] A. Kumar, S.J. Williams, S.T. Wereley, Microfluid. Nanofluid. 6 (2009) 637–646.
[26] J.A. Fagan, P.J. Sides, D.C. Prieve, Langmuir 20 (12) (2004) 4823–4834.
[27] J.A. Fagan, P.J. Sides, D.C. Prieve, Langmuir 21 (5) (2005) 1784–1794.
[28] J.A. Fagan, P.J. Sides, D.C. Prieve, Langmuir 18 (21) (2002) 7810–7820.
[29] S.R. Yeh, M. Seul, B.I. Shraiman, Nature 386 (6620) (1997) 57–59.
[30] W.D. Ristenpart, I.A. Aksay, D.A. Saville, Phys. Rev. E (2004) 69. 2.
[31] G. Schwarz, J. Phys. Chem. 66 (12) (1962) 2636.
[32] J.D. Hoggard, P.J. Sides, D.C. Prieve, Langmuir 24 (7) (2008) 2977–2982.
[33] J. Santana-Solano, D.T. Wu, D.W.M. Marr, Langmuir 22 (13) (2006) 5932–5936.
[34] F. Nadal, F. Argoul, P. Hanusse, B. Pouligny, A. Ajdari, Phys. Rev. E 65 (6) (2002) 8.
[35] A. Castellanos, A. Ramos, A. Gonzalez, N.G. Green, H. Morgan, J. Phys. D-Appl. Phys. 36 (20) (2003) 2584–2597.